Optical Characterisation of Diesel, RME and Kerosene Sprays by Microscopic Imaging

T. T. Shoba, C. Crua*, M. R. Heikal, Martin Gold
1: Centre for Automotive Engineering, University of Brighton, UK
2: BP Global Fuels Technology, Pangbourne, RG8 7QR, UK

Abstract

The spray formation and breakup of fossil diesel, biodiesel (RME) and kerosene was investigated experimentally on a common rail diesel injector using a long working distance microscope. The objectives were to further the fundamental understanding of the processes involved in the initial stage of diesel spray formation, and the influence of viscosity, lubricity and surface tension. Tests were conducted at atmospheric conditions and on a rapid compression machine.

Analysis of the fuel sprays at the start of injection revealed jets for each fuel whose morphology was governed by their Reynolds and Weber numbers. As the fuel viscosity was one of the most varying properties this produced jets that were dynamically different. The differences were also reflected in the injection timing of the fuel sprays where the friction between the fluid and the nozzle wall controlled the start of injection (SOI). Kerosene was found to advance the SOI when compared to the diesel and as such suspected to have an impact on the combustion phasing. The RME results fully corroborated with the conclusions drawn based on kerosene.

Downstream from the nozzle the stabilising effect of viscosity can be seen to reduce the formation of surface waves, ligaments and droplets prior to the reaching the breakup length. It is speculated that the liquid core of the RME jet does not generally breakup directly into ligaments and droplets, but transitions into liquid sheets which then breakup or recombine into ligaments through surface tension.

Introduction

With current climate change issues there is strong interest in biodiesel as a cleaner source of fuels for diesel cars. The EN590 regulation (the physical properties all diesel fuel must meet to be sold in the European Union) allows the blending of up to 7% fatty acid methyl esters (FAME), the main molecule found in biodiesels, with conventional diesel. Across the globe countries are making the addition of biodiesel blends mandatory as a result of continual pressure from consumers in the attempt to reduce CO_2 emissions. Yet the literature available on the effect of these blends on the flow properties and spray formation at realistic engine operating conditions, can often be conflicting. Furthermore, much of the research available considers the fuel blends in a cause and effects method, rarely investigating the effect of fuel physical properties on the fundamental processes involved in the initial formation of sprays. This is due to the difficulty involved in the experimentation techniques to isolate the specific fuel properties that characterise the breakup of sprays.

The importance of the problem of spray breakup for various applications is well recognized and has been extensively studied experimentally and theoretically [1-9]. A rigorous theory of spray breakup would be very complex as it would need to involve modelling of nozzle flow, cavitation, instabilities, the initial formation of ligaments and droplets and their subsequent breakup, evaporation, the entrainment of air and the effects of turbulence [4]. Experimental characterisation of the initial stage of diesel jet formation and primary breakup under realistic engine conditions is challenging due to the harsh environment in which they take place. This inherent complexity is compounded by the highly transient nature of the processes involved, along with the elevated velocities and the microscopic scale at which they occur. Direct visualisation techniques are invaluable to improve the fundamental understanding of primary breakup but because of the challenges posed by the conditions under which diesel jets occur, simplified experiments are often used to infer breakup characteristics at normal operating conditions. In particular, the injection and gas pressures are often reduced, the injector geometry simplified, and the fuel replaced by a model fluid, for safety or dynamic similarity.

Microscopic imaging experiments of diesel sprays have been reported in the literature [6, 10-13], although with varying degrees in the quality of the images produced. Satisfactory lighting can be particularly difficult to obtain at microscopic level. High-power short duration laser pulses may seem appropriate, but speckle patterns caused by the combined reflections of such monochromatic light conceal the underlying morphology of the spray, thus significantly degrading the quality of the resulting images and making their interpretation limited. Such optical artefacts can be observed in images recorded by Lai et al. [12], Badock et al. [11] and Heimgärtner & Leipertz [6], for example. Speckle patterns can be avoided by using a spark light instead of a laser, but, al-

* Corresponding author: c.crua@brighton.ac.uk

though short, the duration of the spark flashes are significantly longer than the pulsed laser and can lead to motion blurring at the proposed magnification, even at low spray velocities, unless the exposure can be accurately controlled by the imaging device. The relatively long and random jitter associated with the timing of the spark can also lead to a significant proportion of 'missed' acquisitions which, combined with the long recharge time of the high-voltage electronics, significantly lengthen the experimental work.

Materials and Methods

Experimental setup

The experiment was conducted on a reciprocating rapid compression machine (RCM) based around a Ricardo Proteus single cylinder engine converted to liner ported, 2 stroke cycle operation. The fuel was delivered by a Delphi common-rail system, comprising a DFP-3 high-pressure pump rated at 200 MPa, and a seven-hole DFI-1.3 injector with a VCO type nozzle. The nozzle's orifices were cylindrical with a diameter of 135μm and a length/diameter ratio of 8. The nozzle had an equivalent cone angle of 154°, and the injector was mounted orthogonal relative to the cameras. A detailed description of the test rig is covered by Crua [14].

High resolution shadowgraphic photographs of diesel, RME and kerosene sprays were obtained by spectrally diffusing a high-power laser pulse. A backlit setup was chosen for observing the sprays as it provides an improvement over the side lighting method as the light scattering issues are solved while providing sharper images inherent to the shadowgraph technique. This technique allowed the visualization of jet instability, surface growth and ligament formation.

A second setup was implemented in order to complement the fine spatial information derived from the still images. An ultra high speed camera was used to accurately record the temporal evolution of diesel sprays at microscopic scales, with a second high speed camera simultaneously recording the macroscopic evolution of the complete spray. This allowed precise tracking of the temporal evolution of diesel jets from the actual start of fuel delivery, thus eliminating the timing uncertainty associated with single images. These optical setups described above were covered in detail by the authors in [15].

Fuel samples

The fuels, listed in Table 1, were chosen to obtain a wide range of physical and flow properties. The RME, compared to fossil diesel, has a substantially increased viscosity and lubricity with a small increase in surface tension. Kerosene was chosen for its opposite trend in physical properties compared to RME, which can assist to indirectly substantiate comparisons between RME and fossil diesel.

Table 1. Physical properties of fuels tested

Property	RME	Fossil Diesel	Kerosene
Density at 15°C ($kg.m^{-3}$)	883	837	803
Kinematic viscosity ($mm^2.s^{-1}$)	4.4	3.3	1.2
Surface tension ($dyn.cm^{-1}$)	33.2	29.8	27.7

Results and Discussion

Jet morphology at the start of injection

Figure 1 shows the initial jet formation of the three fuels injected at 40 MPa injection pressure (important for light load and idle stability of engine) into atmospheric conditions. The fossil diesel exits the nozzle as an undisturbed oblate spheroid which was identified as trapped fuel left over from the previous injection [15]. Fresh fuel from the current injection pushes the residual fuel, causing it to eventually lift off the surface of the nozzle. The residual fuel travels further into the chamber, before being disintegrated by the fresh fuel.

Compared to the fossil diesel, the RME jet appears to resist deformation, most likely due to its increased surface tension (11%) and viscosity (36%), which is expected to exert a stabilising force on the liquid fuel. As can be seen in Figure 1 and Figure 2, the residual RME fuel appears to maintain its spheroidal shape for a longer distance, and disintegrates at a later time compared to the fossil diesel.

The residual kerosene fuel exits the nozzle with a more opaque appearance, indicating that the interface between the gas and liquid is more complex and unstable. Ligaments and droplets can be seen to form almost the instant the jet exits the nozzle. When the fresh fuel penetrates through the residual fuel, the disturbances caused result in an inability of the residual fuel to maintain the shape of a spheroid cap. The presence of surface ligaments can be seen on the periphery of the fresh kerosene jet, which were not identified for the fossil diesel or RME. These observations clearly illustrate the stabilising force of viscosity and surface tension on high-pressure fuel jets, and the impact on the formation of ligaments, droplets and jet instability.

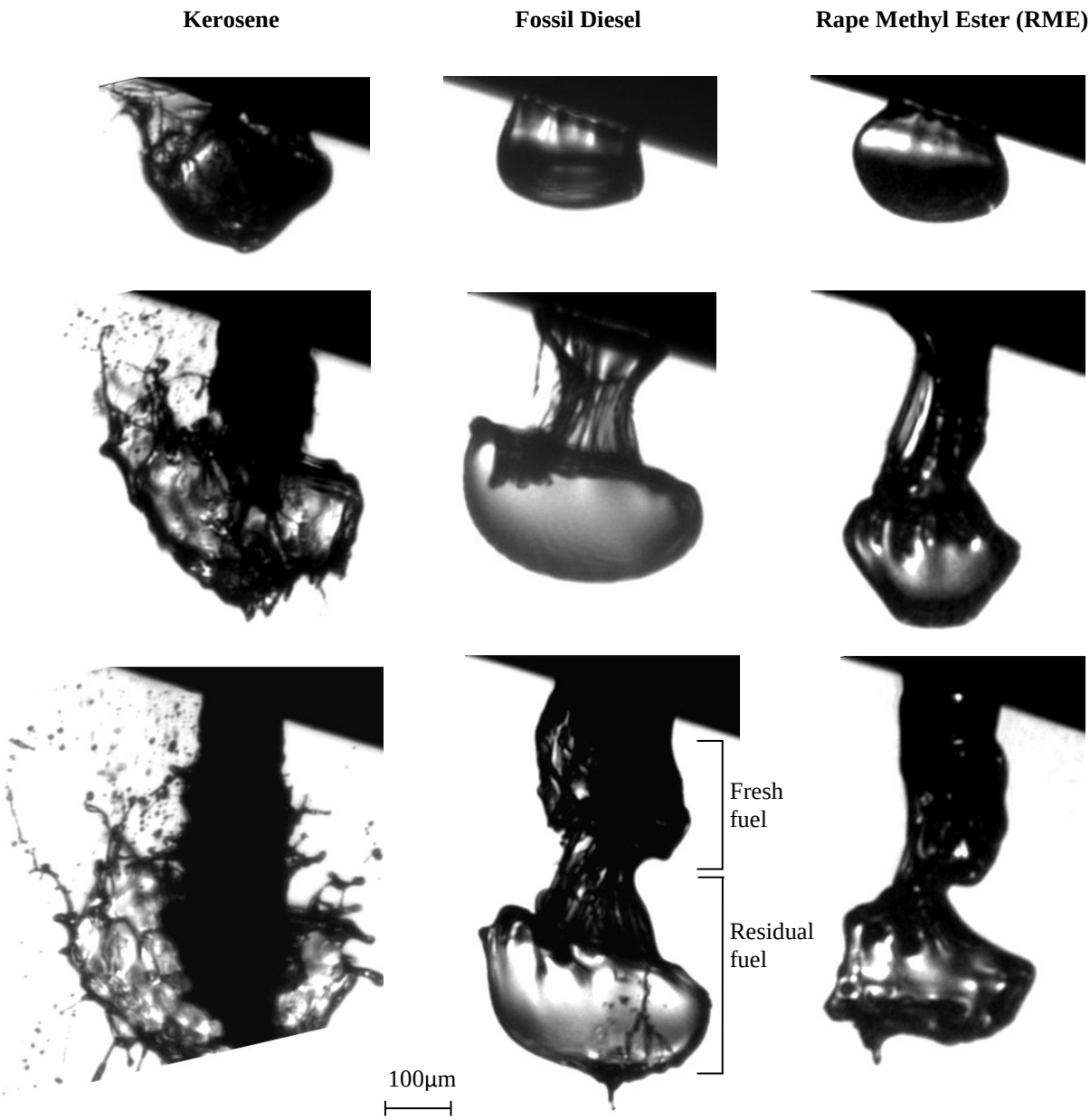

Figure 1. Initial jet formation during the SOI at 40 MPa injection pressure sprayed into atmospheric conditions**.**

These observations tie in when comparing the estimates for the liquid jets' Weber and Reynolds numbers. The balance of inertial and surface tension forces is defined by the Weber number, $We=\rho V^2 d/\sigma$, which can be calculated using either the gas or liquid density. The characteristic length used was that of the nozzle orifice of 0.135mm. As the air inside the rapid compression machine is quiescent [14] it is presumed that the air velocity is zero.

For fossil diesel, with ρ_l the density of the fuel (837 kg.m^{-3}), ρ_g the density of the gas (1.2 kg.m^{-3}), V the exit velocity (Figure 2) of the jet piercing the oblate cap (43.7 m.s^{-1}), and σ the surface tension of the fuel (29.8 dynes.cm^{-1}), We_G is equal to 10.3 and We_L to 7049. Although these Weber numbers cannot be directly compared to the values widely reported for the transitions between breakup modes, they give a relative comparison of the fuel jets' propensity to breakup. The Reynolds number (Re=Vd/ν), a measure of the ratio of inertial forces to viscous forces, can be estimated at 1810. This places the fossil diesel jet in a laminar region but close to the transitional region.The relatively undisturbed appearance of the RME jet is explained by calculating its Reynolds number. Near the orifice at the start of injection the leading edge velocity was measured at 28.3 m.s^{-1}. The Reynolds number is calculated at these conditions as 862 with a We_G of 3.41 and We_L of 2471. This explains the laminar flow observed at the early stages of injection. With this reduced turbulence superimposed with lower Weber numbers there is a reduced rate of droplet formation compared to that of the fossil diesel. The flow rate of RME is reported to be lower than that of diesel fuel [16] resulting in a reduced initial jet velocity which is confirmed by the spray penetration chart shown in Figure 2. The breakup rate is suspected to be further deteriorated by the absence, or reduction, of cavitation due to RME's lower vapour pressure [16]. This reduced rate of atomization was observed throughout the early stages of spray formation.

The data from the ultra high speed images of the kerosene jets corroborate with the values estimated for the fossil diesel and RME. The Re of 4878, We_g of 10.3 and a We_L of 7292 were estimated using the initial velocity of the fresh fuel (43 ms^{-1}). This confirms that the flow is turbulent with a rapid rate of ligament formation.

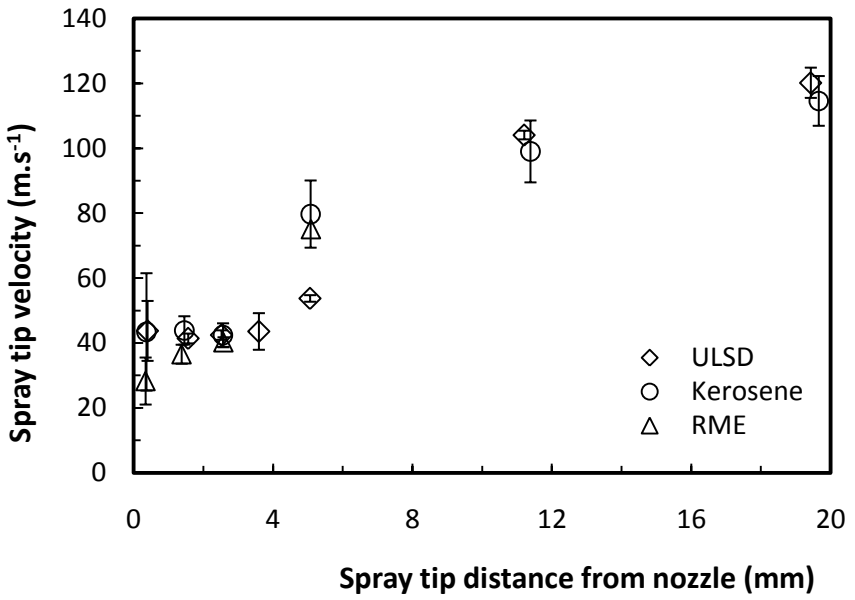

Figure 2. Leading edge velocity for fuels injected at 40 MPa into atmospheric conditions.

Injection timing

By recording the evolution of the fuel jets with an ultra high-speed camera, the evolution of the residual and fresh fuel could be observed through time for single injection events. Figure 3 shows 12 frames extracted from a video recorded at 1280x960 pixels, with 20ns exposures and a fixed interframe delay of 2µs. On these videos the residual fuel has a translucent appearance which can be explained by the relatively undisturbed interface between the liquid fuel and surrounding air, which facilitates the refraction of light towards the camera. The fresh fuel takes a darker appearance, and can be seen emerging from the nozzle at frame 5 in Figure 3. This discontinuity in the refraction of the light allowed the residual and fresh fuel to be independently tracked. Figure 4 shows the evolution of jet tip penetration with time, for kerosene, fossil diesel and RME, derived from these videos. For the RME jet, the residual and fresh fuels were less discernible, hence the distinction between could not be made and the tip of the fresh fuel was not plotted.

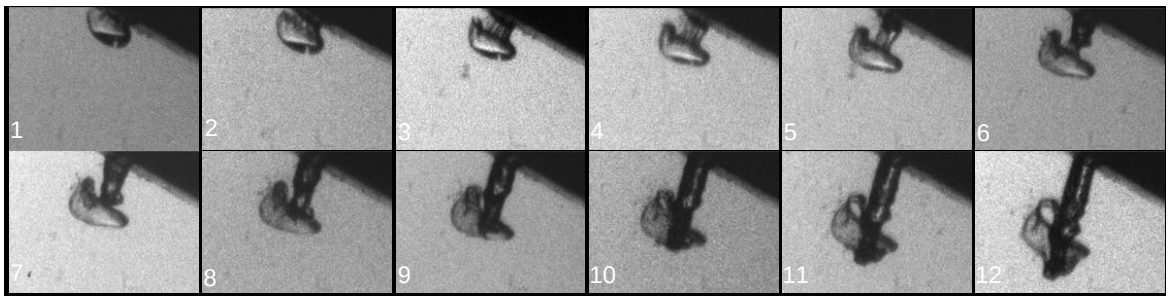

Figure 3. Ultra high-speed video of a fossil diesel jet injected at 40 MPa into atmospheric conditions.

In addition to influencing the morphology of the jets, the fuels were shown to affect the injection timing due to the adhesion between the fuel and the inner nozzle surface. Figure 4 indicates an earlier observed start of injection for kerosene, which was attributed to lower frictional losses between the fuel and the nozzle surface.

RME resulted in a delayed observed start of injection. In spite of its high lubricity, which should reduce friction in the nozzle, the viscosity and surface tension appear to play a more dominant role on frictional losses in the nozzle. Another reason for the delayed injection is that the VCO nozzle opening is more sensitive to RME due to viscosity offering a larger boundary region, hence when the needle is lifting the cross-sectional area being lower than the nozzle holes area results in a delayed flow. This is reflected in the reduced jet velocity observed in Figure 4 attributed to the restricted flow.

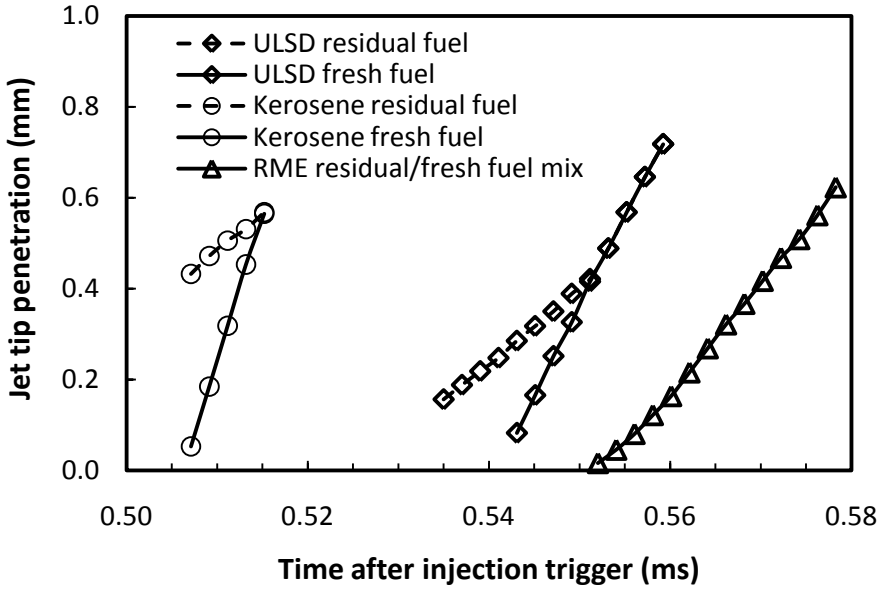

Figure 4. Injection timing of kerosene, fossil diesel and RME fuels injected at 40 MPa into atmospheric conditions. The plots for the fossil diesel were obtained from the video presented in Figure 3.

Jet and spray morphology

As the fuel properties were seen to influence the formation of the jet upon exiting the nozzle it was important to analyse the jets further downstream. Figure 5 shows the effect of fuel properties on the sprays' structures as they undergo the primary atomisation process. At the jet tip penetration for fossil diesel between 0.5 and 1.1mm, the spheroid cap appears pierced and results in a membrane of fuel that trails the leading edge. The effect of aerodynamic forces on atomization have a negligible influence on the breakup of cylindrical jets at low ambient pressures [2], when the ratio of the liquid and gas density is above than 500. Thus for atmospheric ambient pressures, in the region before the onset of breakup, the turbulence of the jet and fuel properties are the key factors that influence initial stages of breakup. With kerosene, the cap does not form a thin membrane. Rather it appears to agglomerate around the jet producing an unstable leading edge that is surrounded with ligaments from which droplets form. In the case of RME, the viscous forces are suspected to resist the formation of ligaments and droplets, resulting in a stabilising effect on the jet. The collapse of the oblate spheroid cap at the leading

edge can be seen to be a sheet-like breakup. The simultaneous increase in viscosity, surface tension and lubricity leads to a notable decreased rate of atomization.

Between 1 and 1.6 mm downstream from the nozzle, soon after the leading edge passes, the lack of ligaments and droplets around the RME jet is clearly evident compared to the fossil diesel and kerosene. The ligaments that are produced from RME are markedly larger than for the other fuels. It is speculated that for high viscosity fuels the breakup of the jet becomes more sheet-like while the surface tension of the fuel pulls the sheets into ligaments. This would explain the reduced presence of droplets and the interconnected nature of the ligaments.

The velocity measurements taken between 1 mm and 2.8mm penetration (Figure 2) produce an average tip velocity that is similar for all fuels. This supports the observations made as the jet is still unbroken; the conclusions made of the Reynolds number at the SOI are valid here, even for the case of RME where the jet speed is faster compared to near nozzle measurements due to the high viscosity of the fuel resulting in a lower Reynolds number. The same conclusion can be made of the liquid Weber number where the higher surface tension would resist the formation of droplets, which is in agreement with the images obtained.

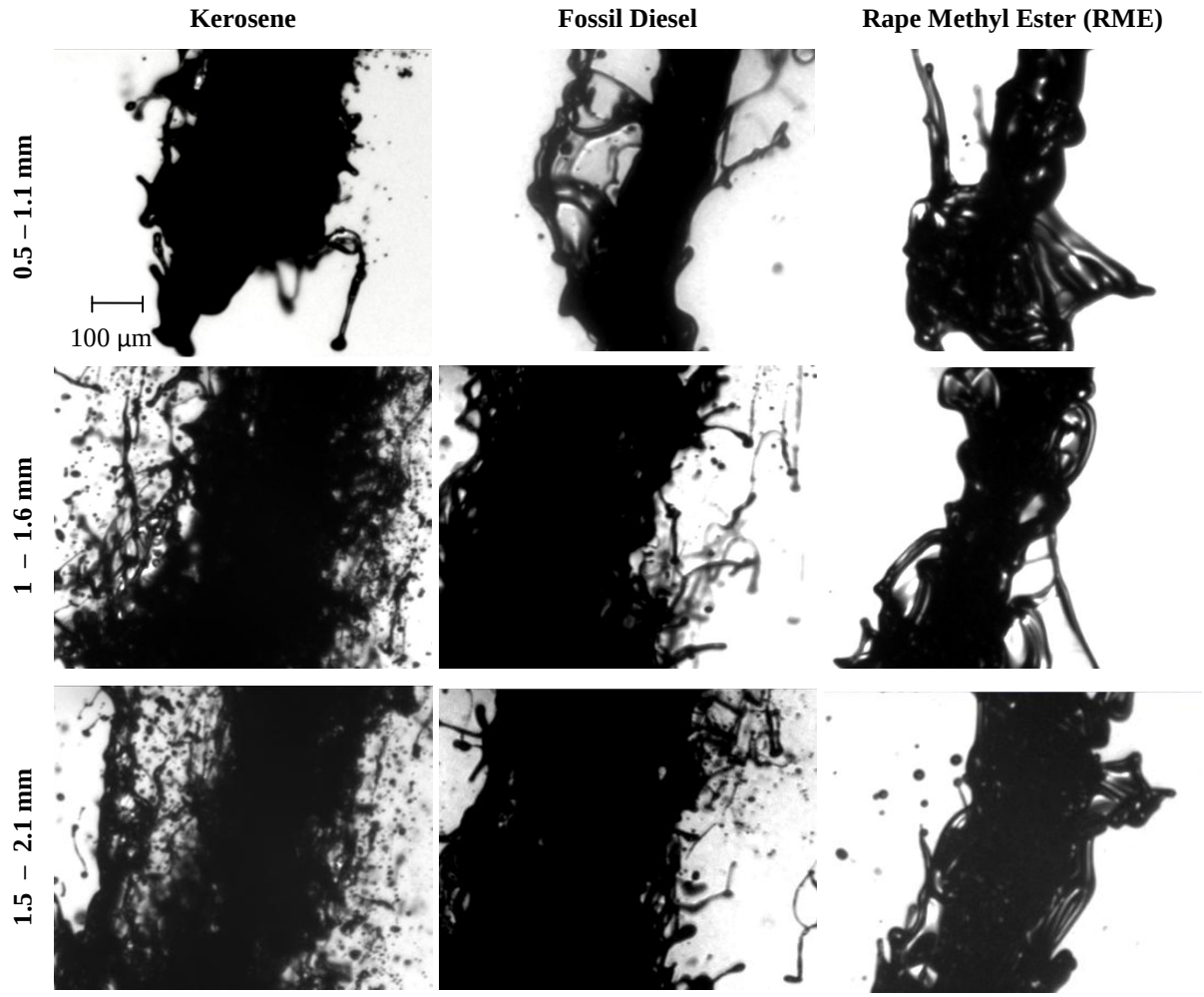

Figure 5. Morphology of the jet at/near the leading edge of the spray up to 2.1 mm below the nozzle. Each row represents the same spatial location.40 MPa injection pressure sprayed into atmospheric conditions.

As the fuel properties play an important role in the initial breakup of the transient jet, the characteristic differences are expected to transfer to the breakup mechanisms involved in the transition to a fully formed spray. During the transformation, the leading edge takes the form of an agglomerated structure where the trailing region consists of ligaments and droplets. Observations made upstream of the spray show that the ligaments are formed directly from the breakup of the liquid core. This breakup of the fuel jet is attributed to the shear aerodynamic forces due to the axisymmetric vortices at the leading edge and the turbulent nature of the jet (inertia supplied

from the high pressure injection) in the form of helical type instability [20]. Ligaments are entrained into the agglomerated tip which continually sustains its existence as it penetrates further into the chamber.

Analysis of the RME sprays directly behind the leading edge at 5.2 mm (Figure 6) reveal a dynamic breakup that is largely different to the other fuels tested. The morphology of the jets at this location consists mainly of intertwined ligaments continuously connected. There is an increased tip velocity and combined with the fuels higher density, an increase in momentum is expected. This suggests that a greater level of breakup should be expected, but there is a distinct lack of droplets and isolated ligaments at this location. An explanation for the breakup observed is that with its higher viscosity and surface tension values, the RME lowers the probability of the formation of detached ligaments and droplets. It is speculated that the liquid core of the RME jet does not generally breakup directly into ligaments and droplets, but transitions into liquid sheets which then breakup or recombine into ligaments through surface tension. This would explain the reduced presence of droplets and the interconnected nature of the ligaments.

Observations further downstream of the nozzle reveal a secondary atomization region dominated by ligaments (Figure 7). The number of droplets is reduced but those present are generally larger. These droplets are more spherical when compared to similar sized droplets produced from the other fuels. This is explained by the higher surface tension which allows the droplets to retain a spherical shape as they resist the formation of new surface area. The lack of breakup at the core also suggests the possibility of less air entrainment and thus reduced shear forces.

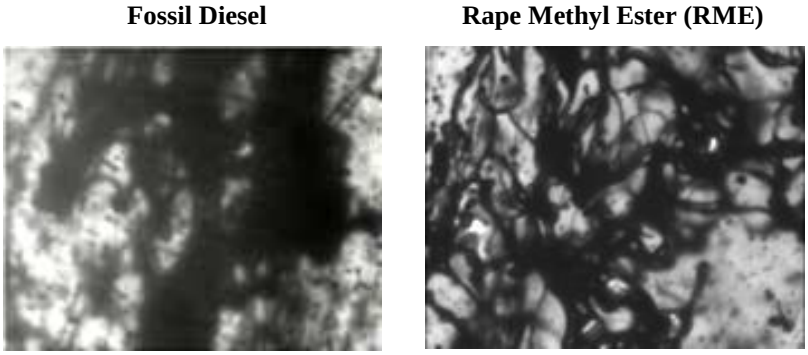

Figure 6. Morphology of the spray behind the leading edge for **fossil diesel** and RME, between 4.6 and 5.2 mm downstream of the nozzle. Injection pressure of 40 MPa into atmospheric conditions.

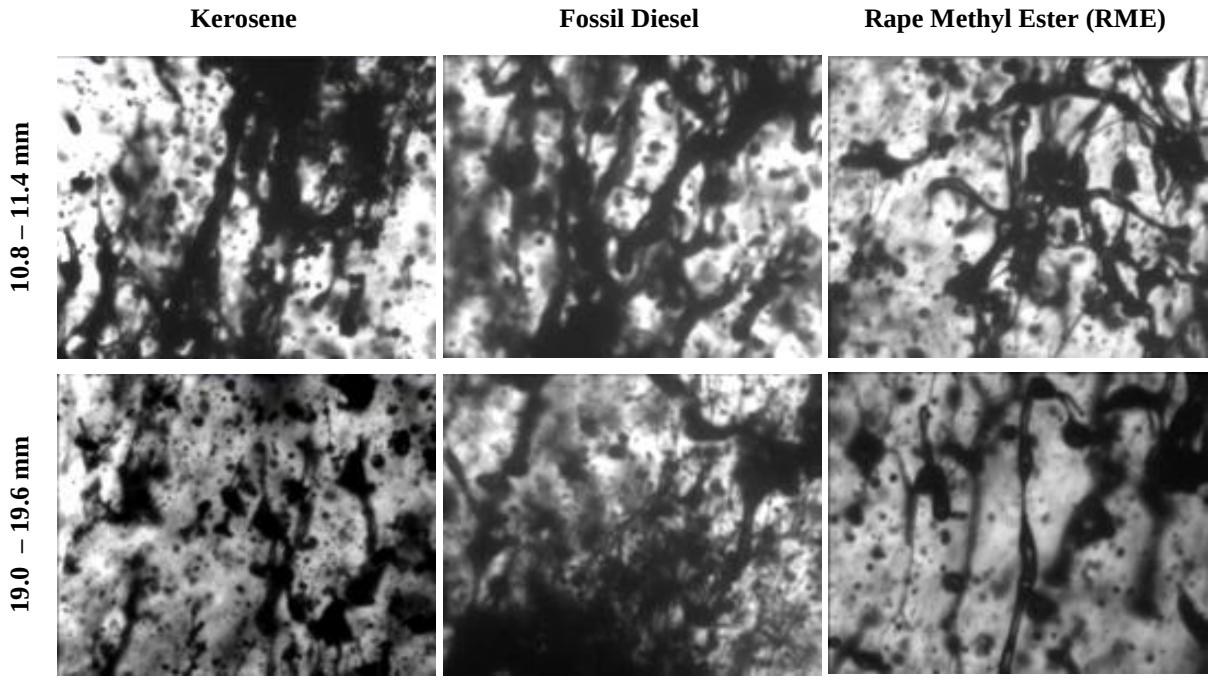

Figure 7. Morphology of the jet behind the leading edge of the spray at 10.8 mm (top row) and 19 mm below the nozzle (bottom row). Injection pressure of 40 MPa sprayed into atmospheric conditions.

Observations of the morphology of kerosene at 10.8 mm downstream from the nozzle reveal a spray that appears similar to the reference diesel (Figure 7). In this region the continuous jet behind the agglomerated leading edge is entering its final stages of primary breakup where droplets and ligaments are forming rapidly. This similarity ends by the time the jet is down to 19 mm from the nozzle. The larger number of smaller droplets with kerosene presents a greater surface area for evaporation.

Conclusions

The morphology of the fossil diesel, RME and kerosene fuels sprays was observed with high spatial resolution. The fossil diesel exits the nozzle as an undisturbed oblate spheroid which was identified as trapped fuel left over from the previous injection.

The dynamics of the initial stage of fuel spray formation were recorded with high temporal and sub-micron resolutions using an ultra high-speed video camera. The evolution of the residual and fresh fuel emerging from the nozzle was observed through time for single injection events, for the fossil diesel, RME and kerosene fuels.

Kerosene exhibited the shortest injection delay, followed by the fossil diesel and RME. The effects of viscosity and surface tension were identifiable when observing the morphology of the initial jet leaving the injector. RME, with its high viscosity and surface tension, resisted the formation of surface waves, ligaments and droplets.

It is speculated that the liquid core of the RME jet does not generally breakup directly into ligaments and droplets, but transitions into liquid sheets which then breakup or recombine into ligaments through surface tension.

Acknowledgement

The authors would like to thank BP International Ltd (GF&LT) and the EPSRC (CASE 07000437) for financial support. The EPSRC Engineering Instrument Pool is acknowledged for supplying equipments.

References

[1] Som, S. and S.K. Aggarwal, *Effects of primary breakup modeling on spray and combustion characteristics of compression ignition engines.* Combustion and Flame, 2010. **157**(6): p. 1179-1193.

[2] Dumouchel, C., *On the Experimental Investigation on Primary Atomization of Liquid Streams.* Experiments in Fluids 45(3), 2008.

[3] Eggers, J. and E. Villermaux, *Physics of liquid jets.* Reports on progress in physics 71(3), 2008.

[4] Faeth, G., Hsiang, L. and Wu, P.,, *Structure and Breakup Properties of Sprays.* International Journal of Multiphase Flow 21(supp 1), 1995: p. 99-127.

[5] Gorokhovski, M. and M. Herrmann, *Modeling Primary Atomization.* Annual Review of Fluid Mechanics 40(1), 2008: p. 343-366.

[6] Heimgärtner, C. and A. Leipertz, *Investigation of Primary Diesel Spray Breakup Close to the Nozzle of a Common Rail High Pressure Injection System.* 2000.

[7] Hossainpour, S. and A.R. Binesh, *Investigation of fuel spray atomization in a DI heavy-duty diesel engine and comparison of various spray breakup models.* Fuel, 2009. **88**(5): p. 799-805.

[8] Lefebvre, H.A., *Atomization and sprays*. Combustion: An International Series. 1989: Taylor&Francis.

[9] Zunping Liu, et al., *Ultra-Fast Phase-Contrast X-ray Imaging of Near-Nozzle Velocity Field of High-Speed Diesel Fuel Sprays*, in *ILASS Americas, 22nd Annual Conference on Liquid Atomization and Spray Systems*. 2010: Cincinnati, Ohio, USA.

[10] Bae, C., et al., *Effect on nozzle geometry on the common-rail diesel spray.* SAE 2002-01-1625, 2002.

[11] Badock, C., et al., *Investigation of Cavitation in Real Size Diesel Injection Nozzles.* International Journal of Heat and Fluid Flow 20(5), 1999: p. 538-544.

[12] Lai, M.-C., et al., *Microscopic Characterization of Diesel Sprays at VCO Nozzle Exit.* SAE 982542, 1998.

[13] Sjöberg, H., G. Manneberg, and A. Cronhjort, *Long-working-distance microscope used for diesel injection spray imaging.* Optical Engineering, 1996. **35**: p. 3591.

[14] Crua, C., *Combustion Processes in a Diesel Engine*, in *School of Engineering*. 2002, University of Brighton: Brighton.

[15] C. Crua, et al., *High-Speed Microscopic Imaging of the Initial Stage of Diesel Spray Formation and Primary Breakup SAE 2010-01-2247*, in *SAE Powertrains, Fuels & Lubricants*. 2010: San Diego, USA,. p. 25-27.

[16] Som, S., et al., *A comparison of injector flow and spray characteristics of biodiesel with petrodiesel.* Fuel, 2010.

[17] Tat, M.E., et al., *The Speed of Sound and Isentropic Bulk Modulus of Biodiesel at 21^{o}C from Atmospheric Pressure to 35 MPa.* 2000.

[18] Tat, M.E. and J.H.V. Gerpen, *Measurements of Biodiesel Speed of Sound and its Impact on Injection Timing*, N.R.E. Laboratory, Editor. 2003: Colorado.

[19] Kegl, B., *Numerical Analysis of Injection Characteristics Using Biodiesel Fuel.* Fuel, 2006. **85**: p. 2377-2387.

[20] Moon, S., et al., *Ultrafast X-ray phase control imaging of high-speed fuel sprays from a two-hole diesel nozzle*, in *ILASS Americas 22nd Conference on liquid atomization and spray systems*. 2010